Phase Compensation in Multi-Pulse N.M.R. Experiments

P. Mansfield * and U. Haeberlen

Abteilung für Molekulare Physik, Max-Planck-Institut für Medizinische Forschung, Heidelberg, Germany

(Z. Naturforsch. **28 a**, 1081—1089 [1973]; received 30 March 1973)

A general scheme is described for self correcting the various coherent phase errors that arise in multi-pulse sequences used for artificial narrowing of the absorption line in solids. The scheme is found to work well experimentally and greatly facilitates the phase alignment procedure by reducing the sensitivity of the multi-pulse response to phase control settings and drifts. First order dipolar terms reintroduced into the average Hamiltonian by the phase errors are also discussed.

1. Introduction

In recent years a number of pulse sequences have been proposed and employed to selectively remove the dipolar interaction in rigid solids, leaving chemical and Knight shifts and electron coupled exchange interactions [1–4]. In order to achieve high resolution it is necessary to use complicated cycles consisting of groups of at least four r.f. pulses in which the effective spin Hamiltonian is switched through reflection symmetry or better still through full symmetry [5, 6].

Finite pulse width and r.f. inhomogeneity effects on the resolution have been previously discussed and compensation schemes described [6–8].

Phase effects of various sorts may also limit the line width resolution by reintroducing first order dipolar terms into the average Hamiltonian. Apart from the question of line width resolution there is the problem of correctly and rapidly setting up these complex sequences. On this point alone it has become apparent that some form of phase compensation in addition to compensation for r.f. inhomogeneity and finite r.f. pulse width effects would be desirable. As will be shown in the experimental section phase compensation does make these cycles less critical to exact phase settings and hence simpler to adjust.

A scheme for the compensation of phase errors has been proposed by Mansfield [6] and its effectiveness was demonstrated in a simple phase alternated sequence [7]. In this paper we wish to show that this method of phase compensation is more general than previously implied, and that it is useful for actual line narrowing experiments.

Reprint requests to U. Haeberlen, Abteilung für Molekulare Physik, Max-Planck-Institut für Medizinische Forschung, *D-6900 Heidelberg*, Jahnstraße 29, Germany.

The principal phase errors can be grouped into the following classes:

(1) Phase errors due to misalignment of the relevant channel phase shifters.

(2) Phase errors arising from current switching phase transients in the transmitter coil at both leading and trailing edges of the r.f. pulse.

(3) Thermal phase drifts, due to slow changes in the electrical properties of both active and passive components during a long pulse sequence.

(4) Random phase jitter. This could also include effects described in (2) if the spectrometer is not both phase and pulse coherent.

The effects described in (3) and (4) have their origin in the electronics and there is little one can do but use conservative component rating in the design and faster gating logic, if these effects are subsequently found to be a serious cause of the residual line broadening.

The errors due to (1) could in principle be removed by careful alignment if the r.f. pulses were pure 90° rotations. This clearly requires sensitive phase control and a great deal of patience. The errors in (2) have recently received some attention by Ellett et al. [9] and by Mehring and Waugh [10] who refer to them as phase "glitches". Under certain conditions they have shown that these errors can be minimized by coherent gating and by careful tuning of the transmitter. More recently Vaughan et al. [11] have described a different procedure for minimizing phase "glitch" effects in multi-pulse experiments.

Improvement beyond this may seem at first sight to be an insurmountable obstacle in the quest for higher resolution in solids. Fortunately, this is not

* Presently on leave of absence from the Department of Physics, University of Nottingham, Nottingham, England.

the case. Not only can phase "glitch" effects be removed but in addition separate phase errors on each of the four channels can be simultaneously compensated by our scheme without affecting the scaling factor.

2. Theory

We describe phase transients, whatever their origin, by a time dependent component of the r.f. pulse which is orthogonal to the main component (c.f. experimental section, Figs. 3 and 4). In all that follows we shall assume:

i) The area under the main part of the pulse, for example the y-component, is much larger than the area under the orthogonal part.
ii) The main part is effectively constant while the pulse is on.
iii) The orthogonal component is zero under steady state conditions.

Failure to meet this last condition in practice implies the presence of a phase misalignment α. This will be separately accounted for.

The effect of phase transients may be treated without specific reference to the electrical details. In the rotating frame the r.f. field Hamiltonian may be written in appropriate units as

$$\mathcal{H}(t) = H_y(t)\, I_y + H_x(t)\, I_x \tag{1}$$

where $H_{x,y}(t)$ are the respective time dependent field components along the x- and y-axes. Of course either component could be the main pulse field in which case the orthogonal component will be the quadrature phase transient field. The Magnus expansion for the pulse rotation operator $P(t)$ may be written [9, 10, 12]

$$P(t) = \exp\{i\,t[\bar{\mathcal{H}}^{(0)} + \bar{\mathcal{H}}^{(1)} + \ldots]\}\,. \tag{2}$$

To this order in the Magnus expansion the resulting effect of the pulse is

$$\begin{aligned} P_{\pm} &\approx \exp\{\pm i\, t_W [a\, I_x + b\, I_y + c\, I_z]\} \\ &= \exp\{\pm i\, t_W\, \boldsymbol{\Omega}\cdot\boldsymbol{I}\} \end{aligned} \tag{3}$$

where

$$a = t_W^{-1} \int_0^{t_W} H_x(t)\, \mathrm{d}t\,, \tag{3a}$$

$$b = t_W^{-1} \int_0^{t_W} H_y(t)\, \mathrm{d}t\,, \tag{3b}$$

$$\begin{aligned} c = (2\,t_W)^{-1} \int_0^{t_W} \mathrm{d}t \int_0^{t} \mathrm{d}t' \,[&H_x(t)\, H_y(t') \\ &- H_y(t)\, H_x(t')]\,. \end{aligned} \tag{3c}$$

$P_{\pm}$ as given by Eq. (3) expresses the net effect of a pulse by a single rotation around the axis $\boldsymbol{\Omega}/|\Omega|$ through an angle $t_W|\Omega| = t_W\sqrt{a^2+b^2+c^2}$. We choose t_W such that $t_W|\Omega| = \pi/2$. In what follows it is more convenient to express the same rotation by a *sequence* of rotations around the axes of reference which contains one pure positive or negative 90°-rotation around the y- or x-axis, e. g.

$$\begin{aligned} P_y = \exp\{-i\,\beta\, I_x\} \exp\{-i\,\gamma\, I_z\}\, R_y \\ \exp\{i\,\gamma\, I_z\} \exp\{i\,\beta\, I_x\} \end{aligned} \tag{4}$$

where $$R_y = \exp\{-i\,\tfrac{1}{2}\,\pi\, I_y\}$$

and $$\tan\beta = c/b\,, \tag{5a}$$

$$\tan\gamma = b/(a\sqrt{1+\tan^2\beta})\,. \tag{5b}$$

Under the conditions (i – iii), β and γ will be small angles and for an *ideal* pulse they would vanish altogether.

We account for an overall phase-misalignment α of a y-pulse, for example, in the following manner

$$\begin{aligned} P_y = \exp\{-i\,\alpha\, I_z\} \exp\{-i\,\beta\, I_x\} \exp\{-i\,\gamma\, I_z\}\, R_y \\ \exp\{i\,\gamma\, I_z\} \exp\{i\,\beta\, I_x\} \exp\{i\,\alpha\, I_z\}\,. \end{aligned} \tag{6}$$

The operator P_{-y} would be obtained by changing $R_y \rightarrow R_{-y}$ only. This follows from $P_{-y}P_y = 1$, where it is assumed that P_{-y} derives from P_y by just reversing $H_y(t)$ and $H_x(t)$. However, in practice generation of P_{-y} will in general change these field components to $H_y'(t)$ and $H_x'(t)$ or alternatively the phases α, β, γ to α', β', γ', so that actual conjugate pairs of pulses no longer contract to the unit operator.

In a similar manner we obtain for x pulses

$$\begin{aligned} P_x = \exp\{-i\,\alpha_1 I_z\} \exp\{-i\,\beta_1 I_y\} \exp\{-i\,\gamma_1 I_z\}\, R_x \\ \times \exp\{i\,\gamma_1 I_z\} \exp\{i\,\beta_1 I_y\} \exp\{i\,\alpha_1 I_z\}\,. \end{aligned} \tag{7}$$

3. Phase Compensation

The pulse timing representation for the reflection symmetry cycle [6, 7] $[\![1, 3, 2; 1, \tilde{3}, 2]\!]$ which is compensated for r.f. inhomogeneity and finite pulse width effects but *not* for phase, is

$$\begin{aligned} [\tau - P_x - \tau - P_{-y} - 2\,\tau - P_y - \tau - P_{-x} - 2\,\tau - P_{-x} \\ - \tau - P_{-y} - 2\,\tau - P_y - \tau\ - P_x - \tau]\,. \end{aligned}$$

We assume that each of the four pulses in the first half of this cycle that is, the $[\![1, 3, 2]\!]$ sub-cycle has a different set of phase errors α, β, γ due to the phase misalignment and/or coherent pulse switching

transients. The lowest order phase errors which appear in the average Hamiltonian are

$$\bar{\mathcal{H}}_{P\varepsilon} = 2\{[(\alpha_1 - \alpha_1') + (\gamma_1 - \gamma_1')]\, I_y + (\beta - \beta_1')\, I_z + [(\alpha_2 - \alpha_2') + (\beta_2 - \beta_2') + (\gamma_2 - \gamma_2')]\, I_x\}\,. \quad (8)$$

where the subscripts 1, 2 refer respectively to the y and x pulses and the prime to the conjugate pulses. The unequal distribution of phase errors associated with I_x and I_y arises from the fact that in the pulse sequence considered P_y and P_{-y} pulses are direct neighbours, whereas P_x and P_{-x} are not. It is clear that $\bar{\mathcal{H}}_{P\varepsilon}$, Eq. (8), would vanish, if the phase errors for the $P_{\pm\alpha}$ pulses were the same. In a well tuned system (see Experimental Section) where at least $\gamma \approx \gamma'$ and $\beta \approx \beta'$ a good deal of cancellation takes place automatically.

(a) The 180° Phase Modulator

In order to achieve phase compensation, the usual phase shifter arrangement is preceded by a 180° phase modulator. The r.f. logic for producing the four pulse phases may be a series (Fig. 1 a) or parallel (Fig. 1 b) arrangement. We denote pulses that pass through the combined phase modulating system

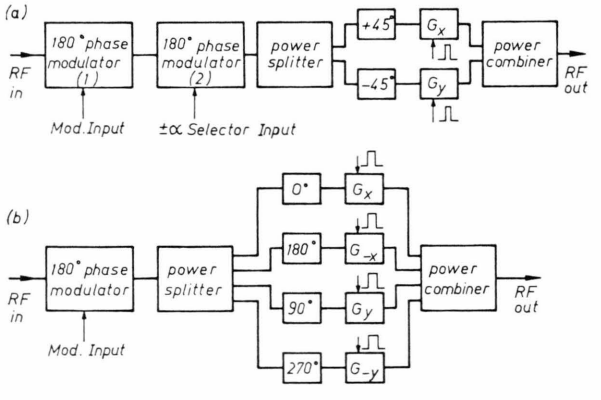

Fig. 1. Simplified phase modulator schemes for phase error compensation. (a) Series phase modulator scheme for producing $P_{\pm x}$ and $P_{\pm y}$ pulses. (b) Parallel phase modulator scheme. Both arrangements are preceded by the additional 180° phase modulator.

but do not pick up the additional 180° phase shift as $P_{\pm\alpha}$ and those that do have the additional 180° shift as $P^{\dagger}_{\pm\alpha}$. Thus if there were no phase errors at all P_α would be formally equivalent to $P^{\dagger}_{-\alpha}$, etc. The compensating procedure is thus to route *all* pulses in a second cycle through the additional 180° shifter. In order to maintain the basic properties of the cycle, however, it is necessary in the following cycle to replace all pulses by their phase complement as above. In this case the fully phase compensated cycle becomes $[\![1, 3, 2; 1, \tilde{3}, 2]\!][\![1, 3, 2; 1, \tilde{3}, 2]\!]^{\dagger}$ where the pulse timing representation of $[\![1, 3, 2; 1, \tilde{3}, 2]\!]^{\dagger}$ is

$$[\tau - P^{\dagger}_{-x} - \tau - P^{\dagger}_{y} - 2\tau - P^{\dagger}_{-y} - \tau - P^{\dagger}_{x} - 2\tau - P^{\dagger}_{x} - \tau - P^{\dagger}_{y} - 2\tau - P^{\dagger}_{-y} - \tau - P^{\dagger}_{-x} - \tau]\,.$$

This latter cycle has the effect of reversing the sign of the phase errors in first order, thereby cancelling the phase errors produced in the first half of the combined cycle. Of course, the very process of introducing an additional 180° phase shift will in general introduce further phase errors, but these are common to all the pulses and therefore also cancel in the second half of the fully phase compensated cycle. The chemical shift scaling factor is unchanged by this phase compensation procedure, and for an ideal cycle would remain at $\sqrt{2}/3$ [6, 7, 13].

(b) Alignment Procedure

The ability to phase compensate a sequence allows a more rigorous alignment procedure with the simpler sequences. For example, for setting the 90° pulse lengths of the x-channel we may now apply the sequence $(P_x - \tau - P^{\dagger}_{-x} - \tau)_n$ maximizing the "double triangle" decay pattern. Other alignments may be similarly performed. Of course one must beware not to try to use a phase compensated sequence to set the phases themselves, for such a procedure could result in the phase concerned being as much as 10° off the desired setting (see for example, discussion of phase compensation in Reference [7]).

4. Inclusion of Spin-Spin Interactions

(a) General

We take the spin-spin interaction Hamiltonian to be

$$\mathcal{H}_1 = \mathcal{H}_D + \mathcal{H}_C + \mathcal{H}_E \quad (9)$$

where the Van Vleck truncated dipolar interaction is given by

$$\mathcal{H}_D = \sum_{i<j} A_{ij}(\mathbf{I}_i \cdot \mathbf{I}_j - 3\, I_{zi} I_{zj}), \quad (9a)$$

the chemical shift interaction is

$$\mathcal{H}_C = \sum_i \delta_i I_{zi} \quad (9b)$$

and the electron coupled exchange interaction is given by

$$\mathcal{H}_E = \sum_{i<j} \tilde{A}_{ij} \mathbf{I}_i \cdot \mathbf{I}_j . \tag{9c}$$

All other symbols have their usual meanings.

Including the effect of $\mathcal{H}_1$ when the r.f. pulse is on, the expression for the r.f. pulse Eq. (3) becomes

$$P = \exp\{i t_W [a I_x + b I_y + c I_z + \mathcal{H}_1 + \mathcal{H}_2]\} \tag{10}$$

where $$\mathcal{H}_2 = d[I_x, \mathcal{H}_1] + e[I_y, \mathcal{H}_1] \tag{11}$$

with

$$d = -i(2 t_W)^{-1} \int_0^{t_W} dt \int_0^t dt' [H_x(t) - H_x(t')] \tag{11a}$$

and

$$e = -i(2 t_W)^{-1} \int_0^{t_W} dt \int_0^t dt' [H_y(t) - H_y(t')]. \tag{11b}$$

Under the conditions (i – iii) d and e will be small compared with unity. Equation (10) may be rearranged using the Dyson separation formula in first order together with the phase generalization embodied in Eq. (7) to give for x-pulses, say

$$\begin{aligned} P_{\pm x} = \exp\{-i\alpha I_z\} \exp\{-i\beta I_y\} \\ \exp\{-i\gamma I_z\} R_{\pm x} \exp\{i t_W [\bar{\mathcal{H}}_1 + \bar{\mathcal{H}}_2]\} \\ \exp\{i\gamma I_z\} \exp\{i\beta I_y\} \exp\{i\alpha I_z\} \end{aligned} \tag{12}$$

where $$\bar{\mathcal{H}}_{1,2} = t_W^{-1} \int_0^{t_W} U^\dagger(t)\, \mathcal{H}_{1,2}\, U(t)\, dt \tag{13}$$

and $$\begin{aligned} U(t) = \exp\{-i\beta I_y\} \exp\{-i\gamma I_z\} \\ \exp\{i |\Omega| t I_x\} . \end{aligned} \tag{13a}$$

Evaluation of Eq. (13) gives

$$\bar{\mathcal{H}}_1 = \bar{\mathcal{H}}_1^{(0)} + \bar{\mathcal{H}}_1^{(1)} \tag{14}$$

where $\bar{\mathcal{H}}_1^{(0)}$ is the average interaction Hamiltonian arising when all phase errors are zero and $\mathcal{H}_1^{(1)}$ is an additional term arising through its explicit dependence on the phase error angles. The first term $\bar{\mathcal{H}}_1^{(0)}$ has been discussed before [6, 14]. The higher order term $\mathcal{H}_2$ also depends on the phase error angles and vanishes for zero phase "glitch" effect.

For notational simplicity we shall put

$$\bar{\mathcal{H}}_1^{(1)} = D_1 + C_1 . \tag{15}$$

Where D and C refer respectively to the dipolar and chemical shift interactions. The terms D_1 and C_1 [Eq. (15)] both vanish when all phase errors are zero.

(b) Dipolar Terms

Evaluation of the dipolar part D_1 gives for x and y pulses

$$\begin{aligned} D_1^{\beta\gamma}(\pm x) = (-6 t_W/\pi) \sum_{i<j} A_{ij} [I_{xi}(I_{zj} \pm I_{yj}) \\ + I_{xj}(I_{zi} \pm I_{yi})] \sum_i \sin\beta \cos\beta \cos\gamma \end{aligned} \tag{16a}$$

$$\begin{aligned} D_1^{\beta\gamma}(\pm y) = (-6 t_W/\pi) \sum_{i<j} A_{ij} [I_{yi}(I_{zj} \pm I_{xj}) \\ + I_{yj}(I_{zi} \pm I_{xi})] \sum_i \sin\beta \cos\beta \cos\gamma . \end{aligned} \tag{16b}$$

For small angles, these correction terms depend only on the angle β. The corresponding properties of this interaction under those pure 90° rotations which are needed are thus

$$\begin{aligned} R_{-x} D_1^{\beta\gamma}(-x) R_x &= -D_1^{\beta\gamma}(x), \\ R_x D_1^{\beta\gamma}(x) R_{-x} &= -D_1^{\beta\gamma}(-x), \\ R_{-y} D_1^{\beta\gamma}(-y) R_y &= D_1^{\beta\gamma}(y). \end{aligned} \tag{17}$$

From these expressions it is straightforward to show that the phase dependent dipolar terms do not cancel over the $[\![1, 3, 2; 1, \tilde{3}, 2]\!]$ cycle. However, the $D_1^{\beta\gamma}(\pm x)$ terms and a substantial part (though not all) of the $D_1^{\beta\gamma}(\pm y)$ terms do cancel for the phase compensated cycle $[\![1, 3, 2; 1, \tilde{3}, 2]\!][\![1, 3, 2; 1, \tilde{3}, 2]\!]^\dagger$ (as well for the $[\![1, 3, 2]\!][\![1, 3, 2]\!]^\dagger$). Some cancellation of the $\bar{\mathcal{H}}_2$ error term also occurs over the $[\![1, 3, 2; 1, \tilde{3}, 2]\!][\![1, 3, 2; 1, \tilde{3}, 2]\!]^\dagger$ cycle.

(c) Effective chemical shift Hamiltonian

The additional chemical shift errors arising are

$$\begin{aligned} C_1^\beta(\pm x) &= t_W \sin\beta \sum_i \delta_i I_{xi}, \\ C_1^\beta(\pm y) &= t_W \sin\beta \sum_i \delta_i I_{yi} . \end{aligned} \tag{18}$$

Since these terms are invariant to rotations about the x and y axes respectively, there is only partial cancellation of them during the cycle, some parts surviving to be included in the scaling factor. Thus for the phase compensated $[\![1, 3, 2; 1, \tilde{3}, 2]\!]$ $[\![1, 3, 2; 1, \tilde{3}, 2]\!]^\dagger$ cycle, the average chemical shift Hamiltonian over the 24 τ period is modified from that given by Mansfield et al. [7] to

$$\begin{aligned} \hbar \mathcal{H}_C = \tfrac{1}{3} \sum_i \hbar \delta_i \{1 + (t_W/2\tau) \\ [(4/\pi - 1 + (2/3)\sin\beta]\} (I_{xi} + I_{yi}) \\ - (t_W/3\tau) \sin\beta \sum_i \hbar \delta_i I_{yi} . \end{aligned} \tag{19}$$

The additional phase dependent term gives a negligible contribution to the scaling factor for $\beta \leqq 2°$.

5. Discussion of Assumptions

In an ideal broad band transmitter, phase "glitches" depend on the gate trigger position with respect to the r.f. waveform. This will be characteristic of a particular gate if the r.f. levels are equal for each channel, a condition not too difficult to achieve in practice. Therefore our scheme will correct for such phase "glitches".

(a) Nonlinear Transmitters

If there are non-linear elements following the r.f. gates it may not be too important as far as phase "glitches" are concerned whether a pulse be P_{α} or $P_{-\alpha}$ since a single ended class C amplifier, for example, does not amplify the negative signal excursions. Phase "glitches" may arise in the post gate electronics and these will be more dependent on r.f. level and pulse length. Whatever the cause, if the actual phase "glitch" seen at the probe head is characteristic of the particular channel, than the cycle can be compensated by the above phase compensation scheme.

(b) Pulse Timing Errors

In a derived coherent system[7] the timing pulses are obtained from an external programmer which gives τ values which are not integral multiples of the r.f. period τ_0. Coherence is achieved by a retiming circuit in which case $\tau = (n \pm 1)\,\tau_0$, n integer. Over a particular cycle, therefore, cancellation of the dipolar Hamiltonian will not in general be perfect and could be a serious source of line broadening. The same considerations apply to a fully coherent system, if the gates are always to open at an r.f. zero crossing for all channels. Fortunately, however, in both systems it is possible to arrange the timing in some cycles (but not in the [1, 3, 2) so that the average dipolar Hamiltonian vanishes and at the same time have coherent gating. In one scheme for the $[\![1, 3, 2; 1, \tilde{3}, 2]\!]$ cycle the timings are

$$[\tau_1 - P_x - \tau_2 - P_{-y} - \tau_3 \; - P_y - \tau_4 - P_{-x} - \tau_5 - P_{-x} - \tau_6 - P_{-y} - \tau_7 - P_y - \tau_8 - P_x - \tau_9]$$

where
$\tau_1 = \tau - \frac{1}{4}\tau_0$, $\tau_6 = \tau - \frac{1}{4}\tau_0$,
$\tau_2 = \tau + \frac{1}{4}\tau_0$, $\tau_7 = 2\tau - \frac{1}{2}\tau_0$,
$\tau_3 = 2\tau + \frac{1}{2}\tau_0$, $\tau_8 = \tau + \frac{1}{2}\tau_0$,
$\tau_4 = \tau - \frac{1}{4}\tau_0$, $\tau_9 = \tau + \frac{1}{4}\tau_0$.
$\tau_5 = 2\tau$,

Clearly a more sophisticated timing logic would be required to produce this sequence.

In a class B or C push-pull transmitter system where all intermediate driver stages are class A or double ended push-pull amplifiers, the leading edge current transients produced in the transmitter coil can be positive as well as negative. In this case there need be no timing error for $P_{\pm\alpha}$ pulses provided all gates and hence waveforms are switched relative to a common point on *one* of the channels, i. e. an r.f. zero crossing for say the P_{-y} channel. In this arrangement the phase "glitch" errors would be minimized for the $\pm y$-channels only. Switching at the $1/\sqrt{2}$ point on the P_{-y} channel waveform would theoretically make all phase "glitch" errors equal. The advantages of any of these schemes are (a) no timing errors, and (b) since all gating is relative to one channel, only one delay and/or trigger circuit is required.

6. Apparatus

(a) Spectrometer

The experiments described were performed on a modified 90 MHz Bruker pulse spectrometer. The main modifications involve the high power r.f. transmitter, the receiver and the probe.

In this spectrometer all gating pulses are coherent with the r.f. carrier, though the trigger positions are arbitrary. Also single ended class C amplification is used in the intermediate stages of the transmitter.

(b) 180° Phase Modulator

The circuit described is a broadband phase modulator and operates from a few MHz up to at least 200 MHz. The scheme of r.f. logic used to generate the 180° phase switching is shown in Figure 2. The circuit is constructed entirely from commercial units.

The r.f. input power (1 v_{pp} into 50 Ω) is split into two components by the power divider (Merrimac, Model P.D.S-20-110). One component serves

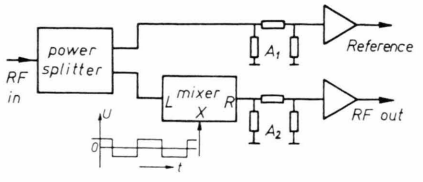

Fig. 2. Diagram of the 180° phase modulator circuit. For details see the text in Section 6 a.

as a reference channel and is fed via attenuator A_1 (9 dB) to the amplifier [Avantek, G.P.D. 402, (12 dB gain)] where its level is restored to 1 v_{pp}. The second component is fed to the L port of a double balanced mixer (Merrimac, Model DMF-2A-500). The output at port R of this device will be in phase or antiphase with its input depending on the sign of the diode bias curent at the modulating input X. The phase modulator r.f. output is fed via attenuator A_2 (6 dB) to a GPD 402 amplifier where its level is restored to ≈ 1 v_{pp}. A simple current switching circuit (not shown) produces the desired phase modulation with a switching time of about 10 ns.

The above circuit was inserted between the spectrometer r.f. source and the input to the three variable phase and one fixed phase channels, as indicated in Figure 1 b.

(c) Phase "Glitches"

Phase "glitches" were studied directly by picking up the r.f. pulses from the probe with a loosely coupled antenna which was connected to the receiver main amplifier. Photographs obtained in this way are shown in Figure 3. Figures 3 a and 3 b show the y pulses together with the phase quadrature components of the x pulses and x pulses together with the phase quadrature components of the y pulses respectively for the $[\![1, 3, 2]\!][\![1, 3, 2]\!]^{\dagger}$ sequence. In each case the 180° phase shift occurs between the fifth and sixth pulse from the left. Since the phase modulator does not produce an exact 180°, (and with our circuit there is no adjustment) it was impossible to get the baseline for all quadrature detected pulses simultaneously equal to zero. However, as mentioned in Sect. 3 the phase correction scheme also corrects for any additional phase introduced by the phase modulator.

Figure 3 c shows the response of four equally spaced pulses P_y, P_x, P_{-x}, P_{-y}. This was obtained by feeding the r.f. via an antenna directly to the broadband phase sensitive detector, and is thus more representative of the actual shapes of the pulses and "glitch" r.f. envelopes.

No noticeable change of the phase „glitch" signals was observed when the gate trigger position was varied with respect to the r.f. carrier waveform. This suggests that the origin of these "glitches" is the post gate amplifier chain.

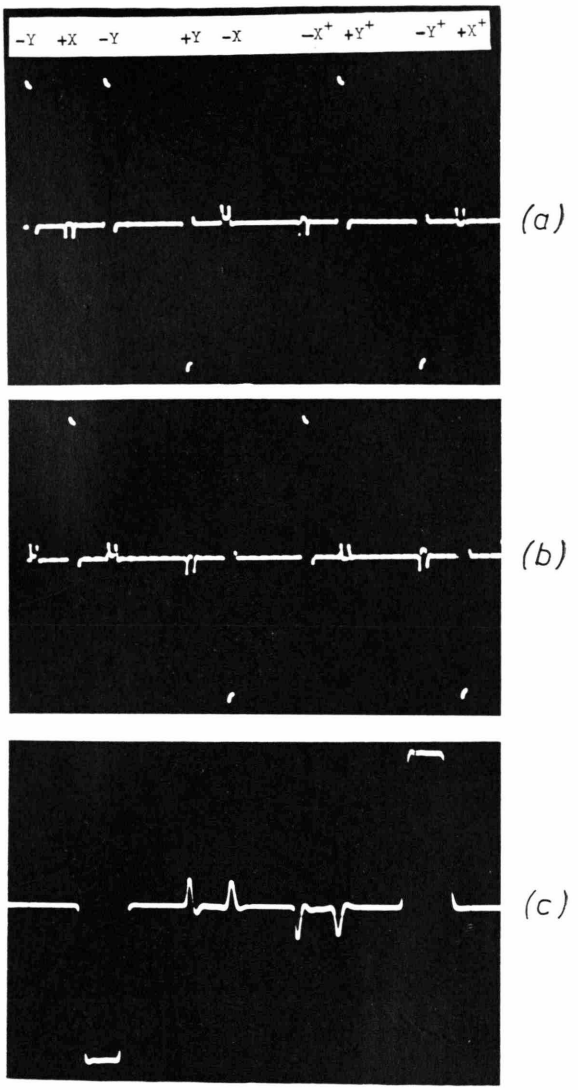

Fig. 3. Photographs of the phase detected r.f. pulses. (a) and (b) show a $[\![1, 3, 2]\!][\![1, 3, 2]\!]^{\dagger}$ pulse sequence with $\tau = 4.0$ μs. In (a) the detector reference phase is adjusted to maximize the P_{-y} pulses, all x-pulses vanishing except for phase "glitches". In (b) the P_x pulses are maximized, all y-pulses vanishing except for phase "glitches". (c) shows an expanded trace of four equally spaced P_y, P_x, P_{-x}, P_{-y} pulses 2.0 μs apart. In this case the pulses were detected directly in the broad band phase sensitive detector whereas in (a) and (b) above, the pulses passed first through the receiver main amplifier before detection. In all photographs the pulses lasted approximately 1.0 μs.

(d) Estimation of Phase "Glitch" Angles

We wish to estimate the magnitude of the angles β and γ occurring in Equation (3). In the case of β, the necessary double integral could, of course, be performed numerically using the waveform of Fig-

ure 3 c. However, it is somewhat more convenient and instructive to evaluate the expression analytically, using empirical functions chosen to approximate the actual observed behaviour. As our model, we take the component functions for $t \geqq 0$ as

$$H_y(t) = H_y[(1 - e^{-lt}) - \Theta(t - t_W)\{1 - e^{-l(t-t_W)}\}], \tag{20}$$

$$H_x(t) = H_x[e^{-mt} + \Theta(t - t_W)\, e^{-m(t-t_W)}] \tag{21}$$

where

$$\Theta(t) = 1 \quad \text{for} \quad t > 0$$
$$= 0 \quad \text{for} \quad t < 0, \quad \text{and} \quad m\, t_W > 1.$$

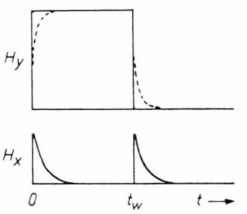

Fig. 4. Sketch of the model pulse and phase "glitch", Eqs. (20) and (21).

We further simplify Eq. (20) by making l large. The functions are sketched in Figure 4. Substituting Eqs. (20) and (21) into Eq. (3 c) we find for $\exp\{-m\, t_W\} \ll 1$

$$c = H_x H_y[2/m^2 - t_W/m]$$
$$= b/2[b\, H_y H_x^{-1} - a]. \tag{22}$$

This last expression comes from substituting expressions for the area under $H_y(t)$ and $H_x(t)$, Equations (3 a and b).

Let the actual areas under the traces in Fig. 3 c be A and B and the corresponding maximum voltages be V_A and V_B. Then since $\alpha\, t_W \approx \pi/2$, we obtain from Eq. (22) and Eq. (5 a)

$$\tan\beta = \frac{c}{a} = \frac{B}{2A}\left[\frac{B}{A}\frac{V_A}{V_B} - 1\right]\frac{\pi}{2}. \tag{23}$$

The quantities in Eq. (23) may be estimated directly from Fig. 3 c and give $\beta = 1.5°$. The angle γ is simpler to estimate since

$$\tan\gamma = b/a = B/A.$$

This gives

$$\gamma = 2.7°. \tag{24}$$

7. Experimental Results

All experiments were performed on ^{19}F in a single crystal of CaF_2 with H_0 along the [111] crystal axis. The signal response was digitally sampled once per cycle and signal averaged over four shots. The data were then Fourier transformed on line. Accurate static magnetic field shifts were obtained by driving the reference of the Bruker external n.m.r. field lock from a frequency synthesizer.

(a) Phase Compensation

The 90° pulse lengths and the relative phases of the four channels were set up approximately using a liquid perfluorobenzene sample. The $\pm\alpha$ pulse lengths were adjusted separately by observing on an oscilloscope the "double triangle" pattern in response to a $(P_{\pm\alpha} - \tau)_n$ sequence. The 90° phase shift between the x and y pulses and the phase sensitive detector reference phase were set using a $P_x - (\tau - 180_y - \tau)_n$ sequence and observing the resonse slightly off resonance. The signal amplitude on either side of the 180° pulse discontinuity is carefully equalized and should remain so independent of frequency.

At this stage of adjustment, the $[\![1, 3, 2]\!]$ or $[\![1, 3, 2; 1, \tilde{3}, 2]\!]$ sequences are highly susceptible to small changes in the phase controls. With the phase compensation switched in, we have found the multipulse response for both cycles to be substantially independent of all phase settings for variations of up to ±3°. On resonance, where the response should be a monotonic decay we found a slow oscillation with a period of about 5 ms. This was independent of all phase and pulse width controls, as one might expect, and is presumably due to a higher order phase or pulse width correction term.

(b) Scaling Factor

The scaling factors for the phase compensated $[\![1, 3, 2; 1, \tilde{3}, 2]\!][\![1, 3, 2; 1, \tilde{3}, 2]\!]^{\dagger}$ and $[\![1, 3, 2]\!][\![1, 3, 2]\!]^{\dagger}$ sequences were measured in the following way. Four count averages of the signal response at a number of equally spaced static field settings upfield from resonance were compounded in the signal averager. The compound decays were Fourier transformed producing a multiple line spectrum, Figure 5. Similar results were obtained downfield. The frequency spacing of the multiple spectrum is in steps of 900 Hz. The line width resolution varies slightly over the 4.5 kHz frequency range but is typically 70 Hz, with the narrower lines closer to resonance. This phenomenon is not attributable to the phase compensation since a similar effect has been observed for the $[\![1, 3, 2; 1, \tilde{3}, 2]\!]$ cycle.

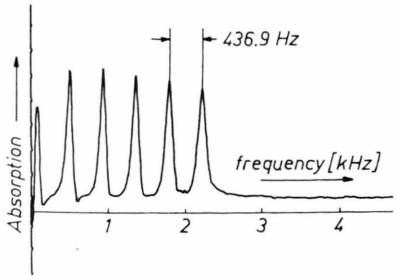

Fig. 5. Graph plotter output of the compounded spectrum of six separate absorption lines recorded at different frequencies in a single crystal of CaF_2 with H_0 along the [111] crystal axis. Each line is narrowed using the fully compensated $[\![1, 3, 2; 1, \tilde{3}, 2]\!]\,[\![1, 3, 2; 1, \tilde{3}, 2]\!]^{\dagger}$ cycle ($\tau = 4.0$ μs) and equally spaced by 900 Hz upfield from resonance. Note the indicated frequency spacing is reduced by the scaling factor 2.07.

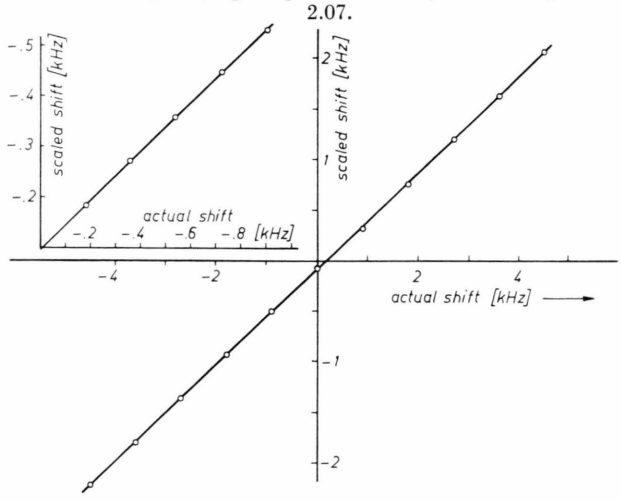

Fig. 6. Graph of actual frequency shift versus scaled shift for data similar to that shown in Figure 5. The inset corresponds to line shifts very close to resonance. In both curves the scaling factor is 2.07. The small offset at zero frequency is *not* a phase effect but is due simply to the fact that the true resonance position was not precisely determined.

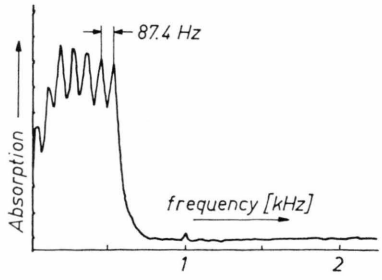

Fig. 7. Graph plotter output of a "just resolved" compound spectrum comprising seven lines equally spaced by 180 Hz. Each line is narrowed by using the fully compensated $[\![1, 3, 2; 1. \tilde{3}, 2]\!]\,[\![1, 3, 2; 1, \tilde{3}, 2]\!]^{\dagger}$ cycle ($\tau = 4.0$ μs) on a single crystal of CaF_2 with H_0 along the [111] crystal axis. Note that the indicated frequency spacing is reduced by the scaling factor 2.07.

A graph of the observed line shift versus the actual frequency shifts is plotted in Fig. 6 and gives a scaling factor of 2.07. An entirely independent experiment gave a scaling factor of 2.06. These values are to be compared with the theoretical value [6, 7] of 2.06.

To check the behaviour closer to resonance, the above experiment was repeated with a frequency interval of 180 Hz. The resulting spectrum is shown in Fig. 7 and depicts a "just resolved" set of lines. The scaling factor in this case is 2.07.

(c) Resolution

A comparison of the line width at fixed τ ($= 4.0$ μs) for the $[\![1, 3, 2; 1, \tilde{3}, 2]\!]\,[\![1, 3, 2; 1, \tilde{3}, 2]\!]^{\dagger}$ and $[\![1, 3, 2]\!]\,[\![1, 3, 2]\!]^{\dagger}$ cycles was made over the frequency range ± 5 kHz about resonance. The line width with the $[\![1, 3, 2; 1, \tilde{3}, 2]\!]\,[\![1, 3, 2; 1, \tilde{3}, 2]\!]^{\dagger}$ cycle was found to be 70 Hz whereas for the $[\![1, 3, 2]\!]\,[\![1, 3, 2]\!]^{\dagger}$ it was 100 Hz, both values unscaled. Thus there is a marginal advantage in resolution for the former cycle. We also found that whereas the former cycle narrows nearer resonance the latter broadens.

We might mention here that we have observed line widths as narrow as 40 Hz for the $[\![1, 3, 2; 1, \tilde{3}, 2]\!]$ sequence. However, when properly examined for scaling factor and symmetry about resonance, the sequence has been found to be misaligned in some way. Use of phase compensation has certainly given consistent results and would seem to obviate any phase misalignment pitfalls.

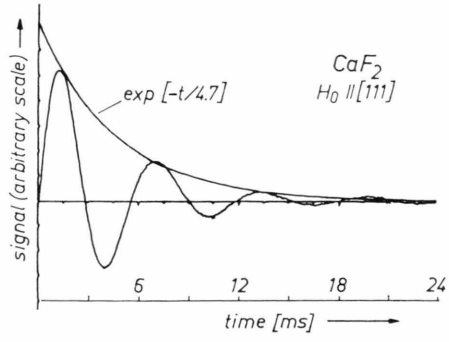

Fig. 8. ^{19}F response to the $[\![1, 3, 2; 1, \tilde{3}, 2]\!]\,[\![1, 3, 2; \tilde{1}, 3, 2]\!]^{\dagger}$ cycle 900 Hz upfield from resonance in a single crystal of CaF_2 with H_0 along the [111] crystal axis. The response is sampled once per cycle and the average of four shots drawn on a graph plotter. The cycle sampling point was arranged to display the signal component which oscillates about zero baseline. The decay of the signal is compared with an exponential function.

An additional practical advantage of the $[\![1, 3, 2; 1, \tilde{3}, 2]\!][\![1, 3, 2; 1, \tilde{3}, 2]\!]^{\dagger}$ cycle is that one component of the response oscillates about zero signal baseline, thus obviating baseline substraction problems in the Fourier transformation. In Fig. 8 is a graphplotter output for such a signal shifted 900 Hz from resonance. Also plotted is an exponential function. The rather good fit to the decaying amplitude demonstrates the Lorentzian nature of the multi-pulse lineshape. In this example the line width is 67 Hz.

8. Conclusions

We have shown both theoretically and experimentally that systematic phase errors occurring in four independent r.f. pulses in the alignment of multi-pulse sequences may be compensated automatically by appropriately phase modulating the r.f. carrier of the pulses. It is shown that phase "glitch" errors are also removed by the same process. In our case, the origin of these phase "glitches" is in the post gate amplifiers, since variations of the gate trigger position with respect to the r.f. carrier waveform produces no noticeable variation of the "glitches".

The phase stability of the spectrometer was considerably improved using the compensation scheme and the spectrometer could be used from day to day without readjustment.

No discernible improvement or worsening in line narrowing was obseverd using phase compensation. Our calculations show that the phase errors reintroduce first order terms into the average Hamiltonian which, for small angles, depend essentially on β. It would thus seem worth continued effort to further reduce or eliminate phase "glitches" altogether.

A small but definite improvement in line narrowing of the $[\![1, 3, 2; 1, \tilde{3}, 2]\!][\![1, 3, 2; 1, \tilde{3}, 2]\!]^{\dagger}$ sequence over the $[\![1, 3, 2]\!][\![1, 3, 2]\!]^{\dagger}$ cycle was observed, the former producing a 70 Hz line width and the latter 100 Hz (unscaled) for $\tau = 4.0$ μs measured between the half height points and both on CaF_2 with H_0 along [111]. At 90 MHz and accounting for the scaling factors, these widths give a resolution of 1.5 ppm and 2.0 ppm respectively.

The $[\![1, 3, 2; 1, \tilde{3}, 2]\!]$ cycle is, of course, compensated for r.f. inhomogeneity and finite pulse width effects whereas the $[\![1, 3, 2]\!]$ cycle is not. This means that all preliminary adjustments can be made with a liquid sample in the former cycle whereas with the latter cycle final trimming of the pulse length must be done on the solid in order to obtain the greatest narrowing.

The scheme described has been used in a study of the proton resonances in a number of organic solids, the results of which are currently being prepared for publication.

Acknowledgments

A grant from the Deutsche Forschungsgemeinschaft for the equipment used in this work is gratefully acknowledged. One of us (P. M.) wishes to acknowledge the kind hospitality of Prof. K. H. Hausser and the Max-Planck-Gesellschaft.

[1] J. S. Waugh, C. H. Wang, L. M. Huber, and R. L. Vold, J. Chem. Phys. **48**, 662 [1968].
[2] J. S. Waugh, L. M. Huber, and U. Haeberlen, Phys. Rev. Letters **20**, 180 [1968].
[3] M. Mehring, R. G. Griffin, and J. S. Waugh, J. Chem. Phys. **55**, 746 [1971].
[4] R. G. Griffin, J. D. Ellett, M. Mehring, J. G. Bullitt, and J. S. Waugh, J. Chem. Phys. **57**, 2147 [1972].
[5] P. Mansfield, Phys. Letters **32 A**, 485 [1970].
[6] P. Mansfield, J. Phys. **C 4**, 1444 [1971].
[7] P. Mansfield, M. J. Orchard, D. C. Stalker, and K. H. B. Richards, Phys. Rev. **B 7**, 90 [1973].
[8] The finite pulse width effect may be removed by a modification recently proposed by M. Mehring, Z. Naturforsch. **27 a**, 1634 [1972]; Rev. Sci. Instrum. **44**, 64 [1973].
[9] J. D. Ellett et al., Adv. Mag. Res. **5**, 117 [1971]; [Acad. Press Inc., New York].
[10] M. Mehring and J. S. Waugh, Rev. Sci. Instrum. **43**, 649 [1972].
[11] R. W. Vaughan, D. D. Elleman, L. M. Stacey, W.-K. Rhim, and J. W. Lee, Rev. Sci. Instrum. **43**, 1356 [1972].
[12] W. A. B. Evans, Ann. Phys. New York **48**, 72 [1968].
[13] Experiments using the compensated reflection symmetry cycle have also since been described by W.-K. Rhim, D. D. Elleman, and R. W. Vaughan, J. Chem. Phys. **58**, 1772 [1973].
[14] U. Haeberlen and J. S. Waugh, Phys. Rev. **175**, 453 [1968].